Design of a Methodology to Evaluate the Impact of Demand-Side Management in the Planning of Isolated/Islanded Microgrids

Juan Carlos Oviedo Cepeda [1,*] [iD]**, German Osma-Pinto** [1] [iD]**, Robin Roche** [2] [iD]**, Cesar Duarte** [1] [iD]**, Javier Solano** [1] [iD]**, Daniel Hissel** [2] [iD]

[1] Escuela de Ingenierías Eléctrica, Electrónica y de Telecomunicaciones, Universidad Industrial de Santander, Bucaramanga 680002, Colombia; gealosma@uis.edu.co (G.O.-P.); cedagua@uis.edu.co (C.D.); jesolano@uis.edu.co (J.S.)

[2] FEMTO-ST, CNRS, University Bourgogne France Comte, UTBM, 90000 Belfort, France; robin.roche@utbm.fr (R.R.); daniel.hissel@univ-fcomte.fr (D.H.)

* Correspondence: juan.oviedo@correo.uis.edu.co; Tel.: +57-316-246-6426

Abstract: The integration of Demand-Side Management (DSM) in the planning of Isolated/Islanded Microgrids (IMGs) can potentially reduce total costs and customer payments or increase renewable energy utilization. Despite these benefits, there is a paucity in literature exploring how DSM affects the planning and operation of IMGs. The present work compares the effects of five different strategies of DSM in the planning of IMGs to fulfill the gaps found in the literature. The present work embodies a Disciplined Convex Stochastic Programming formulation that integrates the planning and operation of IMGs using three optimization levels. The first level finds the capacities of the energy sources of the IMG. The second and third levels use a rolling horizon for setting the day-ahead prices or the stimulus of the DSM and the day-ahead optimal dispatch strategy of the IMG, respectively. A case study shows that the Day-Ahead Dynamic Pricing DSM and the Incentive-Based Pricing DSM reduce the total costs and the Levelized Cost of Energy of the project more than the other DSMs. In contrast, the Time of Use DSM reduces the payments of the customers and increases the delivered energy more than the other DSMs.

Keywords: Isolated/Islanded Microgrids; planning; operation; Demand-Side Management

1. Introduction

Despite the efforts of governments around the world, access to electric energy in isolated regions remains a challenge [1,2]. Isolated/Islanded Microgrids (IMGs) could play a significant role in providing power to these areas where extending the utility grid is not economically feasible [3]. The implementation of Demand-Side Management (DSM) in the planning of Microgrids (MGs) reduces total costs, Levelized Cost of Energy (LCOE), and customer payments, or increases renewable energy utilization [4–9]. In this regard, it seems interesting to investigate if the application of DSMs in the planning of IMGs can bring similar benefits. Despite this, there is a paucity of literature exploring how DSMs can affect IMGs' planning and operation.

The implementation of DSM aims to affect the patterns of consumer consumption using direct or indirect strategies [10,11]. Direct strategies are composed of Direct Load Control and Interruptible/Curtailable Programs. In Direct Load Control strategies, there is a remote controller sending signals to customers' appliances, like air conditioners, heating systems, water heaters, or public lighting, on short notice. The signals can turn the appliances on/off, switch tariffs, or inform about current electricity prices. Interruptible/Curtailable Programs offer alternatives as biding

programs, Emergency Demand Response (DR) programs, Capacity Market programs, and ancillary services, such as frequency support [12,13]. Indirect DSMs are composed of pricing programs, rebates/subsidies, and education programs. Pricing programs charge dynamic tariffs for energy, which can be power-based, energy-based, or a combination of both [14,15]. Energy-based tariffs incentivize energy conservation, and, therefore, are desired in IMG applications, where the energy generation is limited [16]. Instead of having a fixed flat rate, dynamic fares vary in time to reveal the actual costs of producing energy. These rates include the Time of Use (ToU) rate, Critical Peak Pricing (CPP), Extreme Day Pricing (EDP), Extreme Day Critical Peak Pricing (ED-CPP), Day-Ahead Dynamic Pricing (DADP), and Real-Time Pricing (RTP). Properly designed tariffs motivate the customers to shift their demand to off-peak periods, when the electricity price is lower and it is more convenient to produce electricity [17].

Some works in the literature explore how DSM affects the planning of MGs. Kahrobaee et al. propose a sizing approach to determine the capacity of a Wind Turbine and a Battery Energy Storage System (BESS) for a smart household considering price variations in the tariffs [18]. The authors designed a three-step process combining a rule-based controller, a Monte Carlo approach, and a Particle Swarm Optimization to perform the sizing of the components. However, the uncoordinated combination of multiple stages and the lack of an optimization formulation for energy management can lead to sub-optimal results. Erdinc et al. [19] aimed to address these drawbacks by providing a Mixed Integer Linear Programming (MILP) formulation to design an optimal energy management strategy. The work considers the seasonal and weekly variations in the load profiles in the presence of a Real-Time Pricing tariff scheme. However, it does not consider how to design the DSM itself and how different DSMs will impact the sizing of the energy sources. Kerdphol et al. propose a sizing approach for BESS using Particle Swarm Optimization to improve the frequency stability of an MG [20]. The work integrates a dynamic DSM considering load shedding of non-critical loads to rapidly restore the system frequency and reduce the BESS capacity. A rule-based controller used for the load shedding and a Particle Swarm Optimization formulation used for the sizing of the BESS prove to be adequate to regulate the frequency of the MG. However, the rule-based controller and the lack of forecast models to anticipate the critical events can lead to sub-optimal results.

Nojavan et al. [21] propose a bi-objective Mixed-Integer Non-Linear Programming (MINLP) formulation to optimally site and size a BESS in an MG considering DSM. The authors designed two optimization objectives to reduce total costs and Loss of Load Expectation. The work uses an ϵ-constraint method to draw the Pareto optimal curve and a fuzzy satisfying technique to find the best solution. Nevertheless, the authors assume that 20% of the load reacts to a Time of Use (ToU) tariff, ignoring the effects of the demand's self-elasticity. Majidi et al. use a Monte Carlo Scenario reduction technique to determine the size of a BESS in an MG [22]. The work considers the effects of uncertainties in the forecasted renewable generated power and forecasted consumption. However, similarly to [21], the authors do not consider how the customers react to the DSM; they assume that 20% of the load will react to a ToU tariff. Amir et al. [23] propose a combined algorithm to find the size and energy management strategy of a Multi-Carrier Microgrid. The work proposes a mathematical model with high sophistication that uses an MINLP formulation to obtain the optimum dispatch strategy and Genetic Algorithms to obtain the capacities of the energy sources. The work measures the changes in the patterns of consumption of the customers considering varying prices for the different forms of energy. The planning of the Multi-Carrier Microgrid considers demand and price growth over a five-year optimization horizon. Nevertheless, this work does not design the DSM. It only considers the effects of the prices of the energy providers on the Multi-Carrier Microgrid.

Planning of IMGs refers to the set of decisions that the planner must make to design an IMG project. Such decisions include: Setting the energy mix, computing the sizing of the energy sources, and defining the energy dispatch strategy, the economic incentives, and the energy tariffs, amongst others [24–26]. This set of decisions has significant consequences on the performance of IMG projects, where high penetration of renewable energy sources can reduce system inertia, thus challenging

system frequency regulation, control schemes, and transient stability [13]. DSMs can partially solve some of the inherent challenges of planning IMGs.

Chauhan et al. propose to compute the sizing of the energy sources of an IMG considering a DSM that reschedules shiftable loads depending on if it is the winter or summer season [27]. The work uses an Integer Linear Programming (ILP) formulation to find the optimal rescheduling of shiftable loads and a Discrete Harmony Search algorithm to compute the sizing. A considerable drawback of the work is that the DSM only focuses on reducing the peak demand while ignoring maximizing exploitation of renewable energy. Amrollahi et al. combine an MILP formulation and the capabilities of HOMER software to compute the sizing of an IMG composed only of renewable energy sources [28]. Due to the lack of dispatchable energy sources, the authors propose the use of a DSM to reschedule shiftable loads. Rescheduling helps to balance mismatch between electric energy generation and consumption. Mehra et al. propose a work to measure the economic value of applying DSM in the sizing of a nanogrid [29,30]. The work considers the dis-aggregation of electrical demand in critical and non-critical appliances. In addition, the work takes advantage of low-cost computation intelligent devices, such as the "utility-in-a-box" solution, to implement active DSM [31]. The authors use an exhaustive search algorithm to determine the capacities of the Photo-Voltaic (PV) system and the BESS. Nevertheless, the work considers the effects of only one kind of DSM over a small-sized grid.

Prathapaneni et al. propose a multi-objective stochastic sizing algorithm that aims to minimize lifetime costs and degradation of the energy sources [32]. The work considers the effects of a DSM that uses shiftable loads, like electric vehicles or pumped hydro storage in an IMG. The work uses an Accelerated Particle Swarm Optimization (APSO) to compute the sizing of energy sources. Despite considering lifetime costs of the IMG and degradation of energy sources, the work considers a basic DSM over reduced amounts of loads that are not always present in IMG applications. Luo et al. propose a sizing methodology for an IMG using a bi-level optimization algorithm [33]. The first level computes the energy sources' capacities, considering the effects of different combinations of public subsidies for the installation of energy sources. The second level performs the dispatch strategy for the energy sources of the IMG using an MINLP formulation. In the second level of optimization, the authors implement a rescheduling mechanism of shiftable loads. A study case shows that DSM reduces installed capacities of the energy sources for the IMG.

Kiptoo et al., similarly to [28], aimed to implement a DSM to balance generation and electricity demand in an IMG only composed of renewable energy sources [34]. The DSMs consider rescheduling shiftable loads. However, the authors aim to improve the work of [28] by adding an electrical demand forecasting module using a Random Forest (RF) regression forecasting approach. The work shows that the proposed methodology reduces the total costs of the IMG project by 12.41%. Rehman et al. used HOMER software to find capacities of energy sources in an IMG [35]. The work considers a DSM capable of rescheduling shiftable loads and uses Simulink to evaluate the operation of the IMG. The use of Simulink allows the authors to design and test a model predictive control. The model predictive control controls the power during grid-connected operation and regulates load voltage in the islanding operation of the MG. Table 1 summarizes the works found in the literature that deal with the integration of DSM in the planning of IMGs, and that highlight knowledge gaps and the characteristics of the present work. It is vital to notice that Table 1 presents only the articles that consider IMGs because they are strictly related to the present work.

Table 1. Summary of the literature review.

Features	2017	2018	2019	2020	Literature Gaps	Proposed Work
Integration of sizing and Demand-Side Management (DSM)	[27,28]	[29,30]	[32,33]	[34,35]		✓
Stochastic optimization formulation			[32]			✓
Study of subsidies impacts over economic feasibility			[33]			✓
Forecasting impacts in the operation				[34]		✓
Validation of operation after sizing				[35]		✓
Tariff setting for Isolated/Islanded Microgrids (IMGs) for economic feasibility					✓	✓
Utilization of tariffs as DSMs in IMGs					✓	✓
Comparison of different DSMs using one test bench					✓	✓
Influence of public subsidies on tariff setting for IMGs					✓	✓

Despite that some of the works found in the literature evaluate the effects of DSM in the planning phase of MGs and IMGs, none of them compare the effects of different DSMs using the same test-bench. The works found by authors do not focus on design and impact evaluation of DSM over total costs and operational aspects of IMG projects. Moreover, few of the works consider the financial aspects of the cooperation between private and public capital to fund IMG projects. Additionally, none of them allow defining tariffs that guarantee the sustainability of the IMG project over time. In this regard, the present article aims to fulfill gaps found in the literature review by providing a methodology capable of:

- Obtaining the optimal sizing and the optimal energy dispatch strategy of an IMG project using a Disciplined Convex Stochastic Programming formulation.
- Obtaining the optimal energy tariffs and stimulus for the DSM to guarantee the financial viability of an IMG project.
- Evaluating the impacts of different strategies of DSMs over sizing, energy management, and costs of an IMG project in a case study.
- Implementing and evaluating different DSMs in the planning of IMGs using the same test-bench.

The formulation uses flat, ToU, CPP, DADP, and Incentive-Based Pricing (IBP) tariffs as DSM strategies. It also proposes a Direct Load Curtailment (DLC) strategy that curtails customers' electrical demand if required.

The formulation assumes that the DSMs modify the patterns of consumption of the customers, which will lead to a change in the capacities of energy sources [36–39]. The results of the application of the methodology provide the optimal size of the energy sources, the optimal energy dispatch, the optimal tariffs, the economic incentives, and the load curtailment. The rest of the article proceeds as follows: Section 2 presents the definition of the problem and the proposed solution. Section 3 presents a case study as an example of the application of the methodology, and Section 4 includes its results and analysis. Finally, Section 5 presents the conclusions of the work and future directions.

2. Definition of the Problem and Proposed Solution

The present work aims to illustrate for planners and policymakers the benefits of applying DSM for IMG planning. For that purpose, the methodology integrates sizing and IMG operation using three different optimization levels, as shown by Figure 1. The first level obtains the sizes of energy sources using a Monte Carlo analysis. The second level uses a day-ahead rolling horizon over the same optimization horizon of the first level to define incentives, tariffs, and load curtailment of each of the strategies of DSM. Finally, the third level simulates the microgrid operation by iterating in the same rolling horizon that the second level uses. The third level performs the simulation to compute the optimal dispatch strategy after weather and demand profiles are known.

The rolling horizon computes one day in advance at each time and rolls over one year. Each day, the second level computes the proper day-ahead DSM stimulus that the third level uses to compute the day-ahead response of the customers. The second level computes these stimuli using day-ahead forecasts of electrical demand. The third level applies the stimulus found in the second level to compute the customers' response. While the first and second level assess the uncertainties in day-ahead forecasts of the demand and in weather variables, the third level assumes perfect knowledge of these variables. This assumption allows the methodology to compute the impacts of errors in forecasts over the DSM performance. The formulation computes the total costs of operation on the third level. Sections 2.1–2.3 present a detailed explanation of each of the levels. Appendix A, present in Table A1 a description of all the variables used in the following sections with their respective names and units.
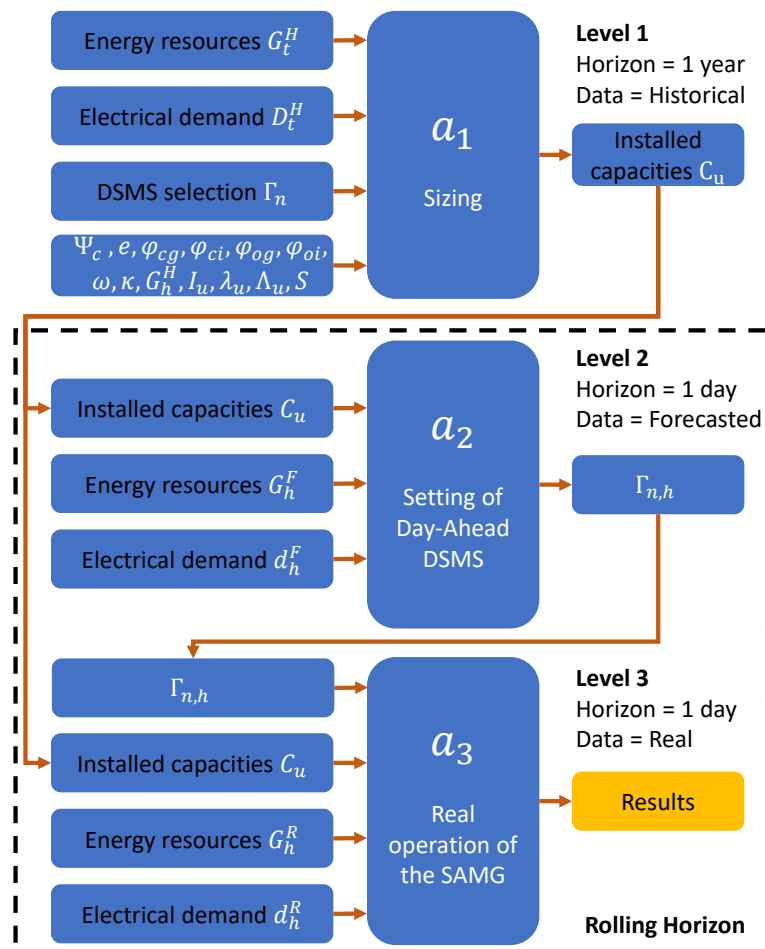

Figure 1. Graphical description of the proposed methodology.

2.1. First Level: Sizing

The formulation of the first optimization level a_1 can be stated as:

$$
\begin{aligned}
J(x^*) = \; &\underset{x}{\text{minimize}} \quad a_1(x, \xi) \\
&\text{subject to} \quad b_i(x, \xi) = 0 \; i = 1, \dots, B, \\
&\qquad\qquad\; c_i(x, \xi) \geq 0 \; i = 1, \dots, C
\end{aligned}
\tag{1}
$$

where x represents the decision variables, ξ represents the uncertainties of the electrical demand, $b_i, i = 1, \dots, B$ are convex functions in x for each value of the random variable ξ, and $c_i, i = 1, \dots, C$ are deterministic affine functions. Since $a_1, b_i, i = 1, \dots, B$ and $c_i, i = 1, \dots, C$ are convex on x, the definition of Formulation (1) is a convex optimization problem [40] ([41], Chapter 7).

IMG projects can receive funding from public or private capital. To compute the effects of the funding sources over the total costs, profits, and customer payments, the formulation of a_1 introduces factors φ_{cg}, φ_{ci}, φ_{og}, and φ_{oi}, where $\varphi_{ci} + \varphi_{cg} = 1$ and $\varphi_{oi} + \varphi_{og} = 1$. The formulation of a_1 is designed to minimize the Capital Expenditures (CAPEX) and the Operational Expenditures (OPEX) of the IMG. Equations (2)–(10) describe the formulation of a_1.

$$
X_1 = \underset{C_u, E_{u,t}}{\arg \min} \; \varphi_{cg} \sum_{u=1}^{U} C_u I_u + \varphi_{og} \sum_{t=1}^{T} \sum_{u=1}^{U} (\lambda_{u,t} + \Lambda_{u,t}) E_{u,t}
\tag{2}
$$

where the CAPEX (ζ) and OPEX (ϑ) refer to:

$$
\zeta = \sum_{u=1}^{U} C_u I_u
\tag{3}
$$

$$
\vartheta = \sum_{t=1}^{T} \sum_{u=1}^{U} (\lambda_{u,t} + \Lambda_{u,t}) E_{u,t}
\tag{4}
$$

and C_u, I_u, $\lambda_{u,t}$, $\Lambda_{u,t}$, and $E_{u,t}$ represent the installed capacity, unitary investment cost, unitary dispatch costs, unitary maintenance costs, and dispatched energy by the u energy source, respectively.

It is worth noting that the formulation of Equation (2) replaces *minimize* with *argmin*, and assigns the results to the variable X_1. This replacement occurs because the second and third methodology levels require the values of the decision variables, but not the value of the achieved minimum. The rest of the optimization formulations in the document maintain the replacement.

The proposed formulation considers the energy prices as the only revenue stream for the investors. Equation (5) introduces a constraint to guarantee that the private investors recover their investments and the expected Internal Rate of Return R.

$$
-(\varphi_{ci}\zeta + \varphi_{oi}\vartheta)(1 + R) + \sum_{t=1}^{T} \pi_{n,t} D_{f,t} \geq 0
\tag{5}
$$

where φ_{ci} and φ_{oi} represent the percentage of payments of the private investor for the CAPEX and OPEX costs, and $\pi_{n,t}$ represents the prices of the n tariff. Equation (6) considers the elasticity (e_t) of the customers at a time t, the initial price of the energy (π_{flat}), and the initial demand ($D_{o,t}$) to compute the final demand ($D_{f,t}$). Equation (7) introduces an energy conservation factor Ψ_c to define how the total energy consumption over the optimization horizon changes after the introduction of DSM. Values of $\Psi_c \leq 1$ decrease the total energy consumption, while values of $\Psi_c \geq 1$ increase the total energy consumption over the optimization horizon. A value of $\Psi_c = 1$ indicates that the total energy consumption over the optimization horizon remains constant after the introduction of DSMs.

$$e_t = \frac{\pi_{flat}(D_{f,t} - D_{o,t})}{D_{o,t}(\pi_{n,t} - \pi_{flat})} \tag{6}$$

$$\sum_{t=1}^{T} D_{f,t} - \Psi_c \sum_{t=1}^{T} D_{o,t} = 0 \tag{7}$$

The formulation of a_1 also includes the energy balance Equation (8), a constraint that limits energy excess (EE_t), and a constraint that limits the lack of energy (LE_t), (9) and (10), respectively. Equations (9) and (10) introduce the parameter z to control the desired level of reliability in the IMG.

$$\sum_{t=1}^{T} \sum_{u=1}^{U} E_{u,t} - EE_t + LE_t - D_{f,t} = 0 \tag{8}$$

$$\sum_{t=1}^{T} EE_t \leq (1-z) \sum_{t=1}^{T} D_{f,t} \tag{9}$$

$$\sum_{t=1}^{T} LE_t \leq (1-z) \sum_{t=1}^{T} D_{f,t} \tag{10}$$

Additionally, the a_1 formulation includes Equations (14) till (26) in order to evaluate the impact of DSM strategies on the sizing of the IMG (changing the horizon from 24 to 8760 h, respectively).

2.2. Second Level: Setting of Day-Ahead DSM Values

The formulation of the second optimization level a_2 solves the following problem:

$$X_2 = \underset{E_{u,h}^F, EE_h^F, LE_h^F}{\arg\min} \; \varphi_{og} \sum_{h=1}^{24} \sum_{u=1}^{U} (\lambda_{u,h} + \Lambda_{u,h}) E_{u,h}^F + \omega EE_h^F + \omega LE_h^F \tag{11}$$

$$s.t. \; \sum_{h=1}^{24} \sum_{u=1}^{U} E_{u,h}^F - EE_h^F + LE_h^F - d_{f,h}^F = 0, \tag{12}$$

where EE_h^F and LE_h^F are the 24 day-ahead forecasted energy excess (a non-positive variable) and the forecasted lack of energy (a non-negative unrestricted variable), respectively, and ω is a penalization factor. $E_{u,h}^F$ and $d_{f,h}^F$ represent the 24 day-ahead forecasted dispatch of the u energy sources and the 24 day-ahead forecasted electrical demand, respectively.

The formulation of the second optimization level a_2 uses the capacities C_u, the day-ahead forecasts of energy resources G_h^F, and forecasts of electric demand $d_{o,h}^F$ as inputs in order to compute the day-ahead stimulus for the five $\Gamma_{n,h}$ DSM strategies. Four of the DSM strategies use π_n in Equation (5) as an indirect stimulus to modify the customer consumption patterns. Those four DSM strategies are: Time of Use pricing (ToU), Critical Peak Pricing (CPP), Day-Ahead Dynamic Pricing (DADP), and Incentive-Based Pricing (IBP). The last DSM uses a Direct Load Curtailment strategy that sheds a percentage of load when required. The baseline case for comparisons uses a flat tariff and no DSM. The description of the baseline case and each of the DSMs proceeds in the following subsections [42].

2.2.1. Flat Tariff (Baseline Case)

In general terms, the unitary value of a flat tariff is the sum of all the costs of producing the energy divided by the total amount of energy produced [43]. Equation (13) describes the yearly payments using a regular flat tariff.

$$\Theta_{flat} = \frac{\zeta + \sum_{t=1}^{T} \vartheta_t}{\sum_{t=1}^{T} D_{f,t}} (1+R) \sum_{t=1}^{T} D_{f,t} \tag{13}$$

However, this traditional approach does not set an optimal tariff to recover investments while minimizing energy costs. Here, we propose the introduction of a decision variable π_{flat} into the formulation to find the optimum price for the tariff.

$$\Theta_{flat} = \pi_{flat} \sum_{t=1}^{T} D_{f,t} \tag{14}$$

2.2.2. Time of Use Tariff

ToU tariffs vary daily or seasonally on a fixed schedule, using two or more constant prices [44]. One of the main benefits of this type of tariff is its stability over long periods, which gives the customer a better ability to adapt to it [45,46]. To create a ToU tariff, the planner must define the number of Y blocks and the starting and ending hours of each y block [45]. The optimization problem considers the prices π_y of the Y number of blocks as decision variables to be computed. Equation (15) presents the yearly payments using Y different block hours of prices.

$$\Theta_{tou} = \sum_{t=1}^{T} \sum_{y=1}^{Y} \pi_y D_{f,t} \tag{15}$$

The methodology computes the ToU and flat tariffs in the first optimization level a_1 and the demand response of the customers in the third level a_3. The second level is not used for the flat tariff and the ToU tariff because they do not have daily variations. The algorithm computes the flat and ToU tariffs following the same process used to find the capacities of the energy sources C_u, using adapted versions of Equations (30) and (31).

2.2.3. Critical Peak Pricing

The CPP tariff can be 3 to 5 times higher than the usual tariff, but is allowed only a few days per year [46]. In Equation (16), π_{base} is a scalar variable that is chosen to be equal to the flat tariff π_{flat}. π_{peak} is a decision variable of dimension 24 and is computed one day in advance. Equation (16) defines the day-ahead forecasted payments using a CPP tariff, and Equation (17) defines the day-ahead hourly critical peak price.

$$\Theta_{cpp}^{F} = \pi_{base} \sum_{h=1}^{\tau_{base}} d_{f,h}^{F,base} + \sum_{h=1}^{\tau_{peak}} \pi_{peak,h}^{F} d_{f,h}^{F,peak} \tag{16}$$

$$\pi_{cpp,h}^{F} = \pi_{base} + \pi_{peak,h}^{F} \tag{17}$$

A critical forecasted event, such as high demand or low generation capacity, triggers the critical peak price in a CPP tariff. In this regard, the CPP tariff must include a predictor of the critical event and a decision mechanism to set the value of the critical price. The first optimization level formulation a_1 uses historical data, which implies that the formulation has full knowledge over the optimization horizon (T = 8760 h). The perfect knowledge allows the formulation to state constraint (18), which limits the apparition of the critical price only to a few hours in a year. Equation (18) uses variable φ_{peak} to control the number of hours with critical price allowed and δ_{peak} to define how many times the base price π_{base} is scaled up. The planner defines φ_{peak} δ_{peak}, and π_{base}, π_{peak}, τ_{base}, and τ_{peak} are decision variables that the optimization formulation computes.

$$\sum_{t=1}^{T} \pi_{peak,t} \leq \varphi_{peak} T \delta_{peak} \pi_{base} \tag{18}$$

However, in order to simulate the operation of the IMG, the rolling horizon will only know the forecasts one day in advance. The formulation must define a mechanism to determine the conditions that allow the critical peak price to take place. Thus, it defines the critical event as low daily forecasted

primary energy resources (lower than a predefined threshold ϱ). The decision mechanism sets the day-ahead value of the critical price using the variable $\pi_{peak,h}^F$. Equation (19) describes the mechanism to set the CPPs in the operational phase of the IMG.

$$\pi_{cpp,h}^F = \begin{cases} \pi_{base} + \pi_{peak,h}^F, & \text{if } \sum_{h=1}^{24} G_h^F \leq \varrho \\ \pi_{base}, & \text{otherwise} \end{cases} \tag{19}$$

2.2.4. Day-Ahead Dynamic Pricing

DADP refers to a tariff that is announced one day in advance to customers and has hourly variations. This scheme offers less uncertainty to customers than "hour-ahead pricing" or "real-time pricing," thus allowing them to plan their activities [47,48]. Equation (20) introduces the day-ahead payments under a DADP tariff, using π_h^F as a decision variable vector of dimension 24.

$$\Theta_{dadp}^F = \sum_{h=1}^{24} \pi_h^F d_{f,h}^F \tag{20}$$

2.2.5. Incentive-Based Pricing

The IBP tariff provides discounts in the tariff to the customers to increase the electric energy consumption or an extra fare to penalize it. The planner can decide the IBP base price to be equal to the flat tariff π_{flat} to guarantee a constant value each day. Variable $\pi_{inc,h}^F$ computes the day-ahead hourly incentives and can take positive or negative values. Equation (21) defines the day-ahead payments using the IBP tariff.

$$\Theta_{inc}^F = \sum_{h=1}^{24} d_{f,h}^F (\pi_{base} + \pi_{inc,h}^F) \tag{21}$$

All of the N tariffs must have restrictions to avoid null or excessive pricing. Governments, policymakers, or IMG owners can guarantee fair tariffs to the customers with constraint (22).

$$\pi_n^{min} \leq \pi_n \leq \pi_n^{max} \tag{22}$$

2.2.6. Direct Load Curtailment Strategy

The DLC strategy curtails a portion ϵ_h^F out of forecasted demand if required. The planner of the IMG decides the percentage of curtailed demand κ. The final demand and day-ahead payments are defined as follows:

$$d_{f,h}^F = d_{o,h}^F - \epsilon_h^F \tag{23}$$

$$\Theta_{dlc}^F = \sum_{h=1}^{24} d_{f,h}^F \pi_{flat} \tag{24}$$

The general restrictions for the DLC strategy are defined as follows:

$$\epsilon_h^F \leq \kappa d_{f,h}^F \tag{25}$$

$$\sum_{h=1}^{24} \epsilon_h^F \leq \kappa \sum_{h=1}^{24} d_{f,h}^F \tag{26}$$

2.3. Third Level: Real Operation of the IMG

The formulation of the third optimization level a_3 solves the following problem:

$$X_3 = \underset{E_{u,h}^R, EE_h^R, LE_h^R}{\arg\min} \quad \varphi_{og} \sum_{h=1}^{24} \sum_{u=1}^{U} (\lambda_{u,h} + \Lambda_{u,h}) E_{u,h}^R + \omega EE_h^R + \omega LE_h^R \tag{27}$$

$$s.t. \quad \sum_{h=1}^{24} \sum_{u=1}^{U} E_{u,h}^R - EE_h^R + LE_h^R - d_{f,h}^R = 0, \tag{28}$$

where the formulation computes the real dispatch of energy sources using capacities C_u, real energy resources G_h^R, real final electric demand $d_{f,h}^R$, and the energy prices π_n of each DSM in order to compute the real dispatch of the U energy sources of the IMG.

In addition to Equations (27) and (28), the formulation of a_3 must include physical restrictions for all the U energy sources used to design the IMG (maximum battery charge and discharge rates, maximum power generator output, amongst others). It is essential to highlight that EE_h^R and LE_h^R in the third level refer to energy that generators produce in excess and energy that the generators can not provide, respectively. The first level constrains the allowed quantity of excess (Equation (9)) and lack (10) of energy. The second level uses a penalization factor for these variables (Equation (11)). However, the third level is just an accumulator, a counter of these quantities.

3. Case Study

The case study aims to illustrate the capabilities and performance of the proposed methodology and considers the design of an IMG composed of a PV, a BESS, and a Diesel Generator (DG) System, as Figure 2 shows. The case study assumes that the microgrid can have two different types of load. The case study uses the load type one when the planner chooses a DSM based on price. The load type one has Smart Meters. The case study uses the second type of load when the planner decides to use the DSM based on DLC. The second type of load has a device as "GridShare" to perform the curtailment of the electrical demand [31]. The case study considers six IMG designs: Baseline case (flat tariff and no DSM) and one design for each of the proposed DSM (ToU, CPP, DADP, IBP, DLC). The results of the designs using DSM are compared with the baseline case design. All of the optimization formulation was written in Python 3.7 using the CVXPY 1.0 package [49,50]. The selected solver is MOSEK, due to its flexibility, speed, and accuracy [51,52].

The case study includes a Monte Carlo Sampling (MCS) approach to deal with the uncertainties of the stochastic formulation. The MCS approach builds different scenarios by sampling the Probability Distribution Functions (PDFs) of electrical demand. In order to build scenarios, a pre-processing step fits the historic electrical demand into monthly/hourly PDFs. For simplicity and for the sake of reduction in computational burden, the case study assumes the demand follows a Gaussian process without a covariance matrix. Afterwards, a random sampling process of the monthly/hourly PDFs builds the demand for each sample s of the MCS approach. Equation (29) describes the sampling process. Figure 3 shows monthly/hourly fitted distributions using a continuous line to represent the mean and a shaded area to represent the standard deviation.

$$D_t|m,h \sim f(\psi_{m,h}) \tag{29}$$

In Equations (2), (11) and (27), X_1, X_2, and X_3 represent the S solutions of minimizing a_1, a_2, and a_3, respectively. The C_u capacities of the energy sources selected for the IMG in the first level must supply 95% of the S electrical demands with z level of reliability (as defined by Equation (10)). A post-processing step fits the C_u results to a PDF ϕ_u, and obtains the Cumulative Distribution Function (CDF) Φ_u. The evaluation of the inverse of the CDF Φ_u at 0.95 provides the values of energy source capacities C_u. These values will supply electrical demand with the desired reliability level 95% of the time (95% of all the scenarios).

$$\Phi_u = \int_{-\infty}^{\infty} \phi_u dC_u \tag{30}$$
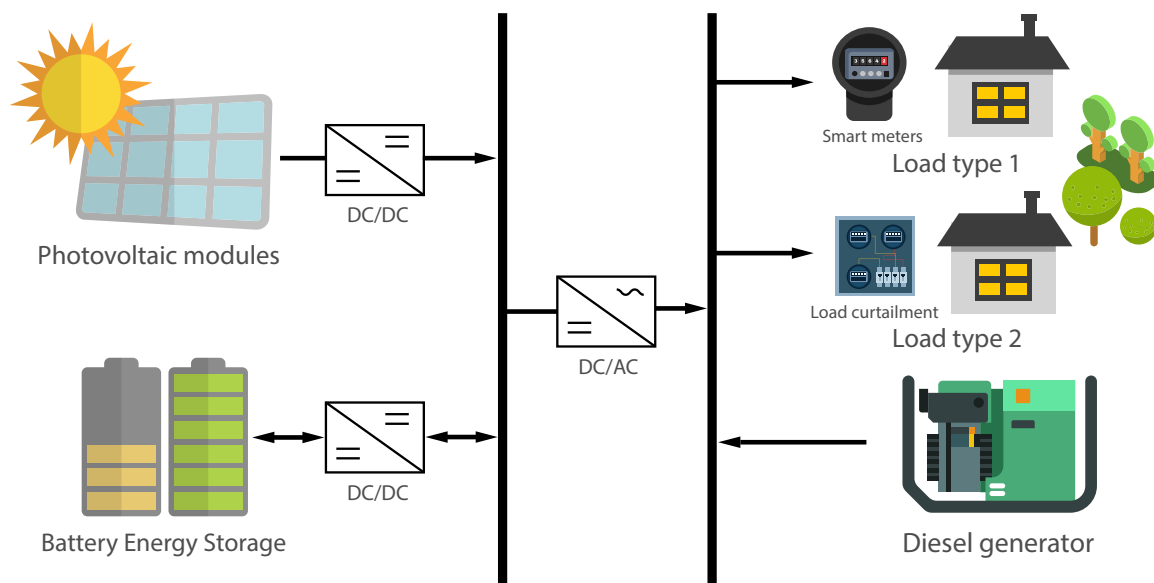
$$C_u = \Phi_u^{-1}(0.95) \tag{31}$$

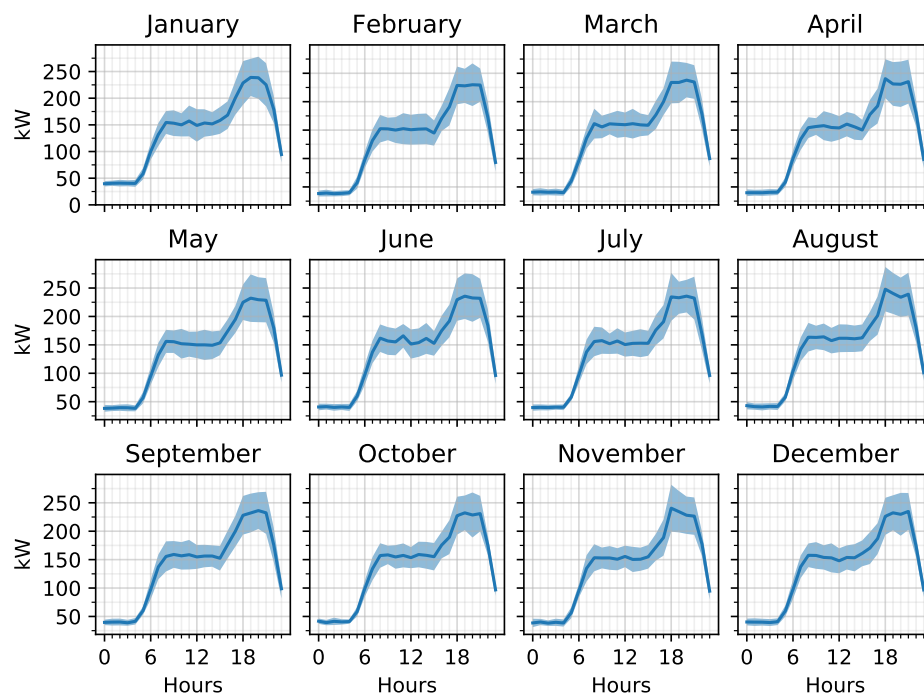**Figure 2.** Architecture of the islanded/isolated microgrid of the case study.

Figure 3. Fitting of the electrical demand.

Geographic and Weather Conditions of the Case Study

The case study is located at longitude $77'16'8''$ West and latitude $5'41'36''$ North (Nuquí, Colombia). The study case uses the Meteonorm database of the PvSyst software to obtain the Global Horizontal Radiation (GHI) and temperature conditions of the geographical region. Additionally, the study case uses Homer Pro software to obtain a standard community electrical demand. The standard community electrical demand that Homer Pro provides has hourly steps over a one-year horizon. Figure 4 shows the historic yearly standard profile of the electrical demand that Homer Pro provides. Figure 5 shows the yearly GHI. Figure 6 shows the yearly temperature.
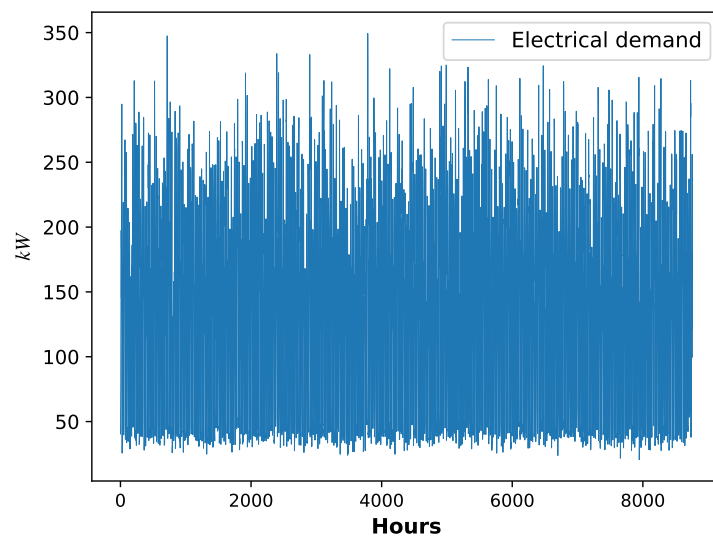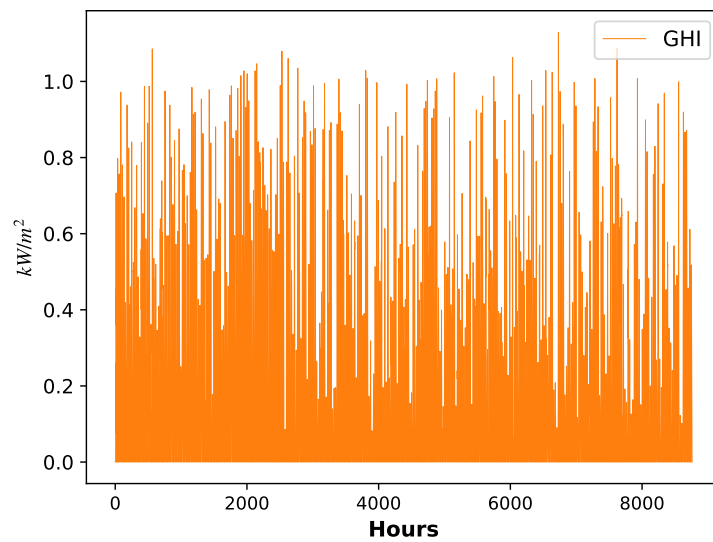
Figure 4. Yearly electrical demand.

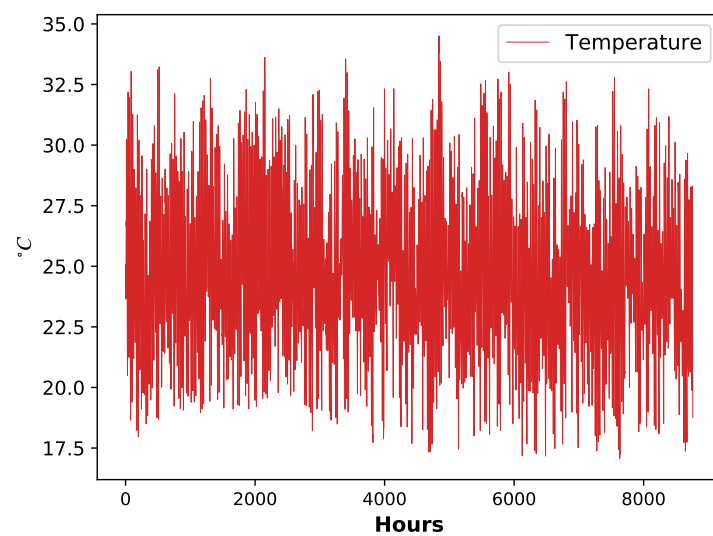**Figure 5.** Yearly Global Horizontal Radiation.

Figure 6. Yearly temperature.

The Monte Carlo Sampling analysis shown in Equation (29) builds the scenarios for the stochastic analysis using the standard community electrical demand obtained from Homer Pro (shown in Figure 4) and a scale factor of 20. The cost of diesel used for the optimization is 0.75 USD/liter. The case study takes the Diesel Generator model from [53], the PV system model from [54–56], and the BESS model from [57]. Table 2 summarizes the unitary installation and maintenance costs of the equipment obtained from regional providers. The values assigned to $\pi_{n,min}$ and $\pi_{n,max}$ in constraint (22) are 0 USD/kWh, and two times the price of the current flat tariff of urban areas in Colombia, 0.34 USD/kWh, respectively [58].

Table 2. Unitary system costs for simulations.

System	Initial Investment	Maintenance	Operation
PV	1300 USD/kW	60 USD/kW	0 USD
BESS	420 USD/kWh	23 USD/kWh	0 USD
DG	550 USD/kW	30 USD/kWh	$f(E_{DG,t}^2, \psi_L)$

Additionally, the methodology takes as inputs the values of Ψ_c, e, φ_{cg}, φ_{ci}, φ_{og}, φ_{oi}, ω, κ, G_h^H, I_u, λ_u, Λ_u, and S. Planners or policymakers can decide these values or perform sensitivity analyses over each of them. Table 3 shows the values used for simulations in this work. The following section uses the MCS approach and the inputs of Table 3 to compute the results and for the case study.

Table 3. Values of the input parameters for the simulations.

Input	Value	Input	Value
Ψ_c	1	κ	10%
e	0.3	G_h^H	Figures 5 and 6
φ_{cg}	0.9	I_u	See Table 2
φ_{ci}	0.1	λ_u	See Table 2
φ_{og}	0.9	Λ_u	See Table 2
φ_{oi}	0.1	S	100
ω	0.4		

4. Results and Analysis

The case study aims to evaluate the effects of five different DSMs over the optimization results of the proposed formulation. The five considered DSMs are ToU, CPP, DADP, IBP, and DLC. The study case evaluates different aspects of the effects of the DSMs. Section 4.1 shows the average of each of the tariffs and the curtailment of the DLC strategy. Section 4.2 shows the effects of the DSMs over the sizing of the energy sources of the IMG. Section 4.3 aims to analyze the impacts of the DSMs over the economic aspects of the microgrid. This section analyzes the impacts of DSMs over total costs, profits of private investors, customer payments, and LCOE. Additionally, the section considers the delivered energy and fuel consumption. Section 4.4 presents the effects of the forecast errors over the operation of the IMG. Section 4.5 presents percentage variations in crucial indicators as total cost of the project and LCOE between the first and the third optimization levels. Finally, Section 4.6 shows a comparison of the performance of all the DSMs.

4.1. Demand Side Management Analysis

Each of the Γ_n DSM strategies uses a different stimulus to modify customer consumption patterns. Γ_{ToU}, Γ_{CPP}, Γ_{DADP}, and Γ_{IBP} use tariffs as an indirect stimulus to modify those patterns. Figure 7 shows the average daily stimulus and the Standard Deviation (STD) of the DSMs. The lines represent daily averages of the DSM strategies, and shaded area represents STDs.
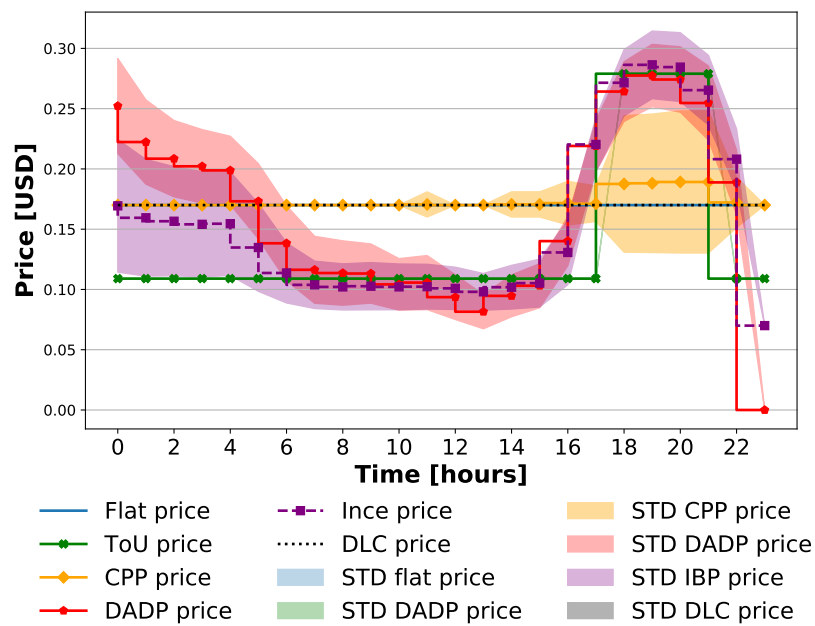
Figure 7. Daily average price of the selected tariffs.

Figure 7 presents energy prices. It is interesting to notice that IBP and DADP tariffs reduce the energy price in the middle of the day. The reduction occurs due to the presence of photovoltaic generation in the IMG. IBP and DADP DSMs incentivize customers to increase energy consumption when it is cheaper to generate electric energy.

The Γ_{DLC} DSM curtails a percentage of the demand. Figure 8 shows the daily average of the curtailed values in a continuous line and the STD of the curtailed energy in a shaded area.
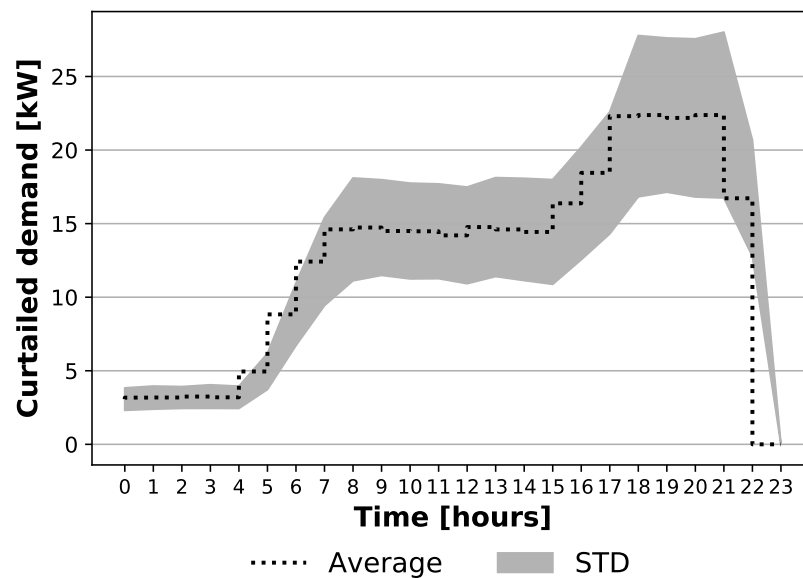

Figure 8. Daily average load curtailment for the Γ_{DLC} DSM.

The stimulus introduced by DSM strategies modifies customers' consumption patterns. Using Equation (6) and the stimulus computed using Equations (15)–(26), it is possible to compute the demand response. Figure 9 shows the demands after the application of DSM. The lines represent daily averages of the electrical demand, and shaded area represents the STDs.
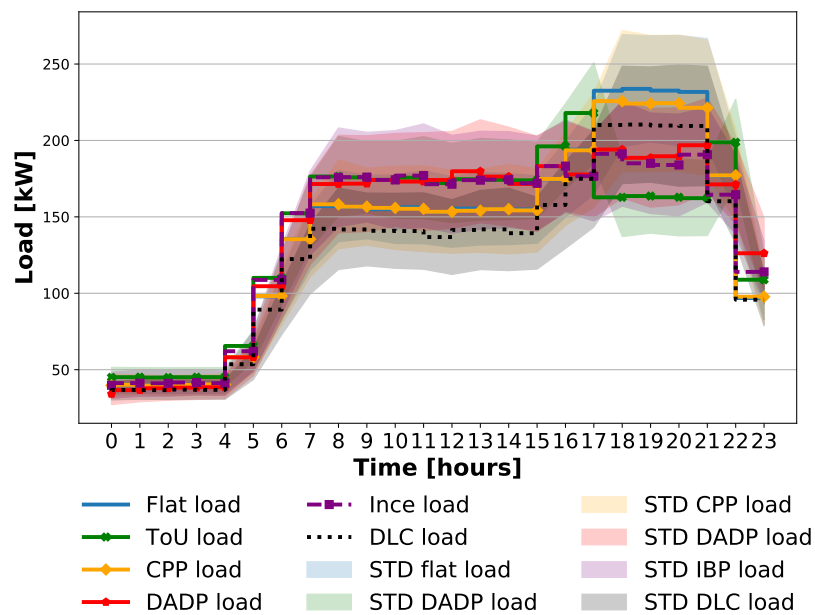
Figure 9. Daily average load for each of the DSMs and the base case.

It is interesting to note in Figure 7 that the IBP rate tends to be similar to the DADP rate. Therefore, it produces similar effects over electrical demand (see Figure 9). The lack of hourly restrictions on the appearance of the incentive of the IBP tariff causes this to occur. However, the design of hourly restrictions will rely on the experience of the IMG planner, which may ultimately lead to sub-optimal results.

4.2. Sizing Analysis

The variations in the customers' consumption patterns modify the IMG sizing. Figure 10 presents the variations in the sizing of the Diesel Generator, the photovoltaic system, and the BESS for the five DSMs.
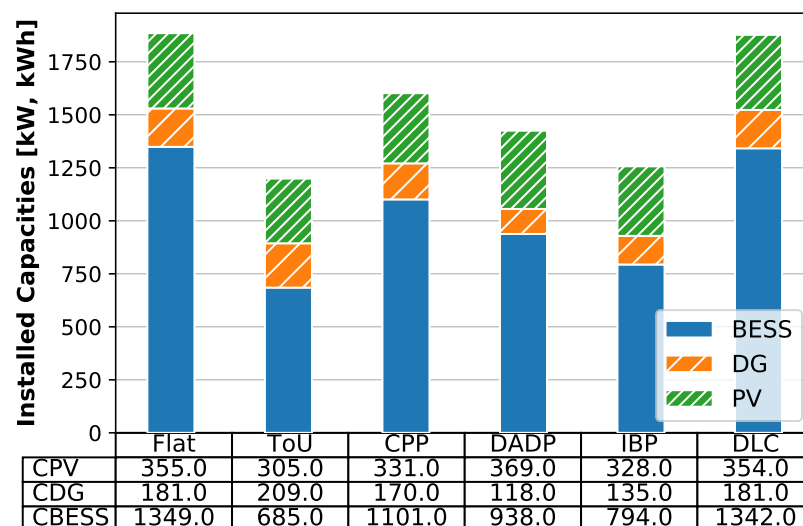

	Flat	ToU	CPP	DADP	IBP	DLC
CPV	355.0	305.0	331.0	369.0	328.0	354.0
CDG	181.0	209.0	170.0	118.0	135.0	181.0
CBESS	1349.0	685.0	1101.0	938.0	794.0	1342.0

Figure 10. Comparison of the sizing of the energy sources for the DSM against the base case. Diesel Generator and photovoltaic capacities are in kW, and the Battery Energy Storage System (BESS) capacity is in kWh.

On the one side, Figure 10 shows that ToU- and IBP-based DSMs require less installed capacity than the other alternatives. On the other side, Figure 10 shows that DLC and CPP DSMs do not considerably reduce the energy sources' installed capacities. However, reductions in installed capacities do not necessarily mean that one DSM is better than others. The following sections contribute with different analyses to determine which of the DSMs can be more suitable for IMG applications.

4.3. Economic Analysis

The DSM introduction in the IMG planning modifies total costs, investors' profits, customers' payments, total delivered energy, and LCOE, among others. Equations (32)–(36) present how to compute these values, and Figure 11 shows the results for the five DSM strategies and the base case.

$$\text{Total costs} = \zeta + \vartheta \tag{32}$$

$$\text{Profits} = \sum_{t=1}^{T} \pi_{n,t} D_{f,t} - (\varphi_{ci}\zeta + \varphi_{oi}\vartheta) \tag{33}$$

$$\text{Payments} = \sum_{t=1}^{T} \pi_{n,t} D_{f,t} \tag{34}$$

$$\text{Energy} = \sum_{t=1}^{T} D_{f,t} - |EE_{f,t}| - |LE_{f,t}| \tag{35}$$

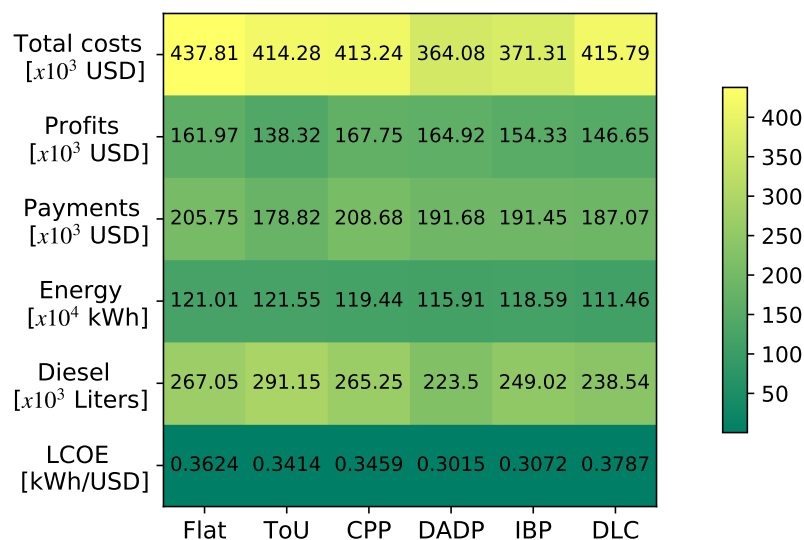$$\text{LCOE} = \frac{\text{Energy}}{\text{Total costs}} \tag{36}$$

Figure 11. Comparison of the costs and the Levelized Cost of Energy (LCOE) of the five DSMs against the base case.

4.4. Assessment of the Impact of Forecast Errors

In the operational stage of the IMG, the proposed formulation computes the DSM stimulus using day-ahead load forecasts. Instead of using a particular method to perform the forecasts, the approach adds Gaussian noise to the real demand to build the forecasted demand, as is stated by Equations (37) and (38). This approach allows measurement of the impact of forecast errors over the final results in the third stage (after knowing the real values of the load).

$$\nu \sim \mathcal{N}(\mu, \sigma^2) \tag{37}$$

$$d_h^F = d_h^R \nu \tag{38}$$

Thus, this section presents a sensitivity analysis of the impact of forecast errors. By computing the simulations again, considering forecast errors of 0%, 5%, 10%, and 15%, this approach computes forecast errors using the Mean Absolute Percentage Error. Table 4 relates the percentage of error with the STD used in Equation (37).

Table 4. input parameters for simulations.

Error	σ^2	Error	σ^2
0%	N/A	5.01%	0.0628
10.01%	0.1258	15.01%	0.1881

It is significant to notice that the reported errors correspond to the average error for all the forecasts of all the simulated scenarios. In the 0% error case, the forecasted demand values are equal to the real values $d_h^F = d_h^R$. The case study found that the methodology is unable to compute the day-ahead stimulus of the DSMs when the forecast errors are near to 20% ($\sigma^2 = 0.2512$).

Figure 12 shows that the impact of the forecast errors in the total costs, the delivered energy, the investors' profits, the customers' payments, and the LCOE is not significant. The variation between the case with perfect forecasts and 15% error in the forecasts is less than 1%. The DADP tariff presents the highest variation in profits and payments of the customers, which drop 1% as compared to the case where the forecast errors are zero.
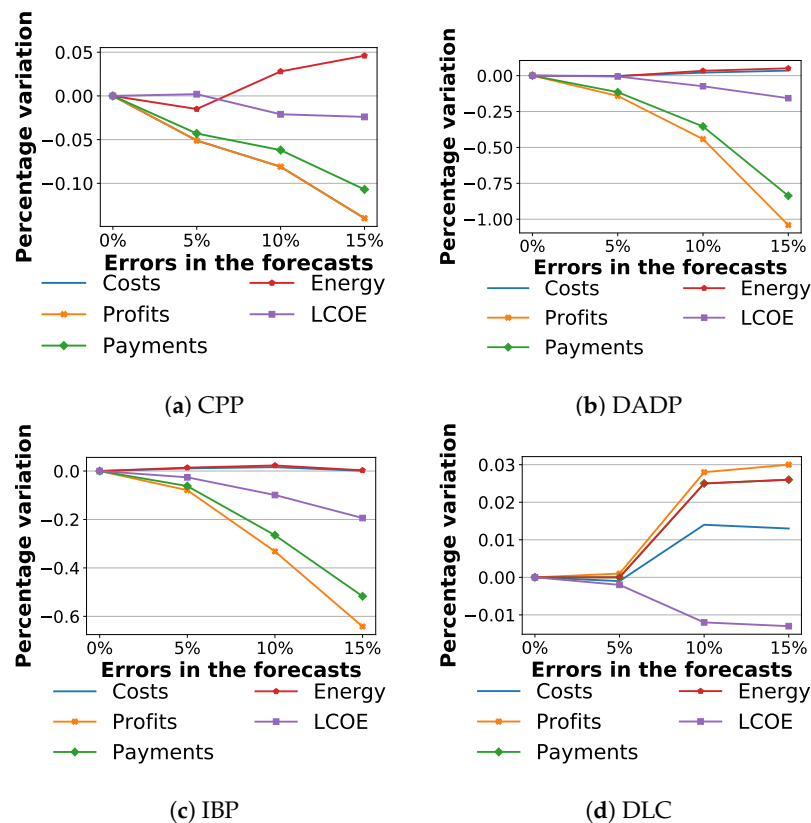

Figure 12. Effects of the forecast errors over the main results. (**a**) Forecast errors effects for a Critical Peak Pricing (CPP) DSM. (**b**) Forecast errors effects for a Day-Ahead Dynamic Pricing (DADP) DSM. (**c**) Forecast errors effects for an Incentive-Based Pricing (IBP) DSM. (**d**) Forecast error effects for a Direct Load Curtailment (DLC) DSM.

4.5. Assessment of the Relation between the First and Third Optimization Levels

This article presents the design of a methodology to compute the effects of five different DSMs over the sizing of IMGs. However, in order to calculate the energy sources' capacities, only the first optimization level of the proposed methodology is required. The second and the third optimization level formulations evaluate the performance of the IMG once it is in operation. Figure 13 reveals the percentage variations between the results from the first and third optimization levels for the five DSMs and the base case.

The first level of the proposed methodology uses a scenario approach built upon historical data and considers an optimization horizon of one year. The second and third levels use a scenario approach built upon forecasts to predict DSMs and consider a rolling horizon with an optimization horizon of one day over a year. Figure 13 presents the comparison between the average results from the first and third levels when the error in the forecasts is 10%. The extra costs, payments, and LCOE, as well as the reductions in profits and payments, are the result of the change of the optimization horizons and the use of historical instead of forecast data. Planners can also compute percentage variations between the first and third levels for different forecast errors and can utilize trends in percentage variations of each of the values to avoid executing the second and third levels of the methodology. Just by executing the first level and considering the percentages' variations in their calculations will be enough to estimate the total costs of the IMG project.
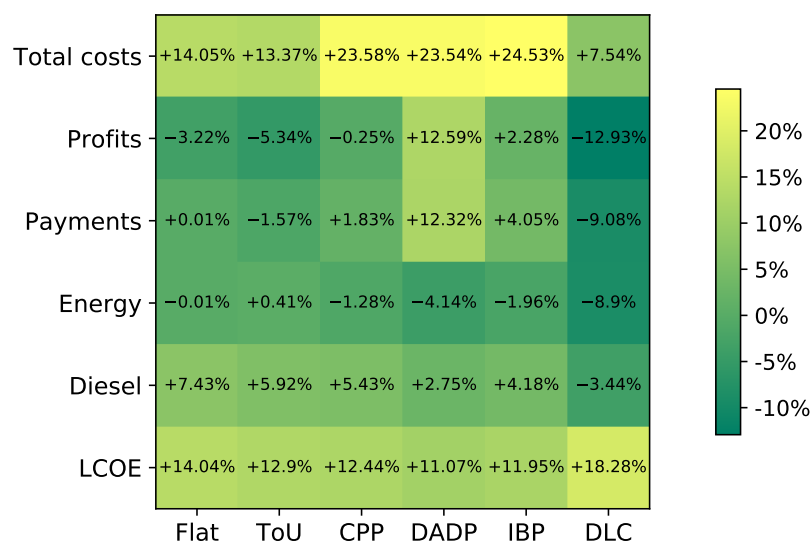

Figure 13. Percentage differences between the results of the first level and the third level for the five DSMs and the base case.

4.6. Performance Comparison of the Five DSMs

The five DSMs have different performance in different aspects. Equation (39) is adopted to measure the performance of each of the DSMs.

$$\text{Performance} = \frac{\text{worst} - \text{current}}{\text{worst} - \text{best}} \tag{39}$$

Figure 14 shows that DADP and IBP tariffs perform better than the other DSMs. However, these rates require announcing energy prices one day in advance, so customers reorganize their consumption daily. In the context of IMG, hourly variations of the tariffs might not be the best option in some scenarios. In those scenarios, a ToU tariff or CPP tariff can give a satisfying solution as well.
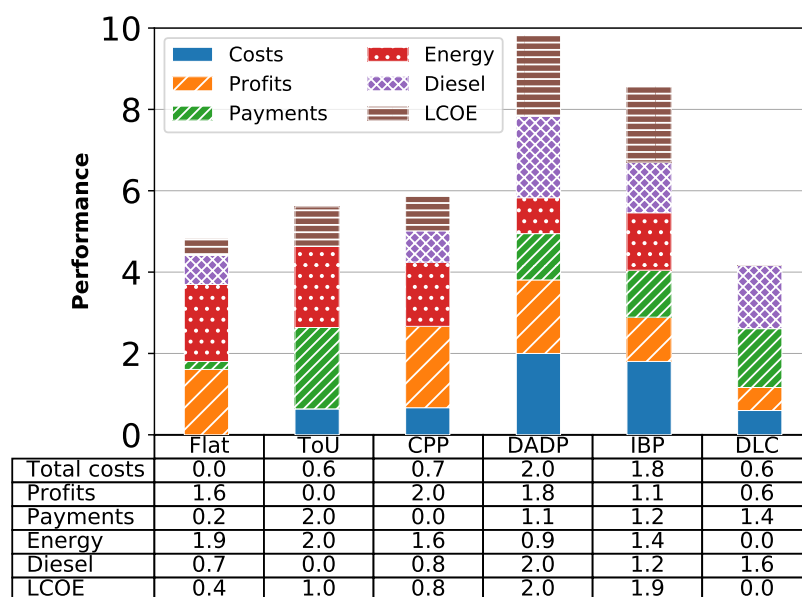
	Flat	ToU	CPP	DADP	IBP	DLC
Total costs	0.0	0.6	0.7	2.0	1.8	0.6
Profits	1.6	0.0	2.0	1.8	1.1	0.6
Payments	0.2	2.0	0.0	1.1	1.2	1.4
Energy	1.9	2.0	1.6	0.9	1.4	0.0
Diesel	0.7	0.0	0.8	2.0	1.2	1.6
LCOE	0.4	1.0	0.8	2.0	1.9	0.0

Figure 14. Performance comparison of the base case and the five DSMs

5. Conclusions

The present work proposes a methodology to design and evaluate five DSMs in the planning and operation of IMGs. The methodology allows determination of the optimal size, optimal energy dispatch strategy, and optimal stimulus for the DSMs using a Disciplined Convex Stochastic Programming approach. The work designs and evaluates the effects of the five DSMs using one case study as a test-bench, which makes this work the first attempt to do so in the literature known by the authors.

The proposed methodology can help policymakers design proper regulations for IMG projects that consider the social conditions of customers and private investors. Additionally, the methodology can be useful for IMG planners or entrepreneurs that want to build profitable business models providing energy to isolated communities. In this regard, the methodology allows policymakers to:

- Compute the effects of applying one of the five DSMs over the total costs of IMG projects in the planning phase.
- Control the revenue of private investors or entrepreneurs to prevent excessive profits.
- Minimize the total amount of subsidies paid by the government for IMG projects.
- Compute the effects over the sizing and the total costs of IMG projects for different values of customer elasticities.

Additionally, the methodology allows IMG planners or entrepreneurs to:

- Compute the expected expenses and revenues of an IMG project considering any of the five DSMs.
- Compute the sizing of the energy sources considering any of the five DSMs.
- Consider the effects of using different combinations of energy sources to supply the electrical demand.
- Obtain the optimal day-ahead energy dispatch strategy for the microgrid considering any of the five DSMs.

The methodology can provide the benefits mentioned above to its users if the assumptions that it was built upon are fulfilled. In this regard, by sharpening the assumptions, the methodology will adapt better to the conditions of IMG projects. Considering more energy sources, sophisticated models of customer elasticities, and demand response models adapted to local conditions, among others, will improve the methodology as well.

Finally, it is essential to highlight the technical characteristic of the present study, which aims to inform planners and policymakers about the benefits of applying DSMs in the planning of IMGs. However, policymakers should perform comprehensive social and behavioral studies to evaluate the potential of acceptance of price-based or direct load curtailment DSMs in the context of IMGs.

Abbreviations

The following abbreviations are used in this manuscript:

DSM	Demand-Side Management
MG	Microgrid
IMG	Isolated/Islanded Microgrid
LCOE	Levelized Cost of Energy
BESS	Battery Energy Storage System
PV	Photovoltaic
DG	Diesel Generator
MILP	Mixed Integer Linear Programming
MINLP	Mixed Integer Non-Linear Programming
CAPEX	Capital Expenditures
OPEX	Operational Expenditures
MCS	Monte Carlo Sampling
PDF	Probability Distribution Function
CDF	Cumulative Distribution Function
STD	Standard Deviation
ToU	Time of Use
CPP	Critical Peak Pricing
DADP	Day-Ahead Dynamic Pricing
IBP	Incentive-Based Pricing
DLC	Direct Load Curtailment

Appendix A

Table A1. Variable declaration.

First stage optimization variables		
a_1	Optimization formulation of the first stage	Unitless
φ_{ci}	Percentage of the CAPEX paid by the investor	Unitless
φ_{cg}	Percentage of the CAPEX paid by the government	Unitless
φ_{oi}	Percentage of the OPEX paid by the investor	Unitless
φ_{og}	Percentage of the OPEX paid by the government	Unitless
X_1	Results of the optimization formulations of the first stage	Unitless
t	Hour of optimization	Hours
T	Total number of hours to optimize	Hours
u	Specific generator or storage system of the microgrid	Unitless
U	Total number of generators and storage systems of the microgrid	Unitless
n	Specific DSM	Unitless
N	Total number of DSMs	Unitless
C_u	Installed capacity of the u device	kW, kWh
I_u	Unitary initial investment of the u device	USD/kW
λ_u	Unitary costs of generation of the u device	USD/kWh
Λ_u	Unitary maintenance costs of the u device	USD/kWh
$E_{u,t}$	Quantity of energy delivered with the u device	kWh
ζ	Total capital expenditures	USD
ϑ	Total operational expenditures	USD
R	Internal Rate of Return for the investors	Unitless
$\pi_{n,t}$	Price of the n tariff scheme at time t	USD/kWh
$D_{f,t}$	Final electrical demand of the community	kWh
e_t	Self-elasticity of the customers	Unitless
π_{flat}	Flat tariff	USD/kWh
$D_{o,t}$	Initial electrical demand of the community	kWh
Ψ_c	Electric energy conservation factor	Unitless
EE_t	Amount of energy in excess	kWh
LE_t	Lack of energy to fulfill the demand	kWh
z	Reliability level	Unitless
Second stage optimization variables		
a_2	Optimization formulation of the second stage	Unitless
X_2	Results of the optimization formulations of the second stage	Unitless
h	Hours of the day	Hours
$E_{u,h}^F$	Quantity of forecasted delivered energy with the u device	kWh
EE_h^F	Amount of forecasted energy in excess	kWh
LE_h^F	Lack of forecasted energy to fulfill the demand	kWh
ω	Penalization factor	Unitless
$d_{f,h}^F$	Final electrical day-ahead forecasted demand of the community	kWh
Θ_{flat}	Payments with flat tariff	USD
Θ_{tou}	Payments with ToU tariff	USD
y	Specific hourly block of the ToU tariff	Unitless
Y	Total number of hourly blocks of the ToU tariff	Unitless
π_y	Price at hour y of the ToU tariff	USD/kWh
Θ_{cpp}^F	Day-ahead forecasted payments of the customers under the CPP tariff	USD
π_{base}	Base price of the CCP tariff	USD/kWh
τ_{base}	Time under base price for the CPP tariff	Hours
$d_{f,h}^{F,base}$	Forecasted final electrical demand at base price	kWh
τ_{peak}	Time under peak price for the CPP tariff	Hours
$\pi_{peak,h}^F$	Forecasted peak price of the CCP tariff	USD/kWh
$d_{f,h}^{F,peak}$	Forecasted final electrical demand at peak price	kWh
$\pi_{cpp,h}^F$	Forecasted Critical Peak Price tariff	USD/kWh
$\pi_{peak,t}^F$	Peak price of the CCP tariff	USD/kWh
φ_{peak}	Percentage of the horizon T allowed to have a peak price	Unitless
δ_{peak}	Times that π_{base} is scaled in the CPP tariff	Unitless
G_h^F	Global horizontal solar radiation	W/m^2
ϱ	Threshold to trigger the CPP price	kW/m^2
Θ_{dadp}^F	Day-ahead forecasted payments of the customers under the DADP tariff	USD
π_h^F	Forecasted hourly price of the DADP tariff scheme	USD/kWh
Θ_{ince}^F	Day-ahead forecasted payments of the customers under the incentive-based tariff	USD
$\pi_{ince,h}^F$	Forecasted incentive price of the IBP tariff	USD/kWh
$\pi_{n,min}$	Minimum value of the n tariff	USD/kWh
π_n	Price of the n tariff scheme	USD/kWh
$\pi_{n,max}$	Maximum value of the n tariff	USD/kWh
$d_{o,h}^F$	Forecasted initial electrical demand	kWh
ϵ_h^F	Forecasted curtailed demand	kWh
Θ_{dlc}^F	Day-ahead forecasted payments of the customers under the DLC DSM	USD
κ	Percentage of the electrical demand to curtail	kWh

Table A1. *Cont.*

Third stage optimization variables		
a_3	Optimization formulation of the third stage	Unitless
X_3	Results of the optimization formulations of the third stage	Unitless
$E_{u,h}^R$	Real quantity of delivered energy with the u device	kWh
EE_h^R	Real amount of energy in excess	kWh
LE_h^R	Real lack of energy to fulfill the demand	kWh
$d_{f,h}^R$	Real final electrical demand	kWh
Case study		
D_t	Electrical demand at time t	kW
m	Months of the year	Unitless
h	Hours of the day	Hours
$\psi_{m,h}$	PDF of the month m and hour h	kW
Φ_u	CDF of the capacity results	kW
ϕ_u	PDF of the capacity results	kW
s	Specific scenario	Unitless
S	Total number of scenarios	Unitless
Y_L	Diesel price per liter	USD/liter
L_u	Lifetime of the u technology	Years
L_p	Lifetime of the IMG project	Years

References

1. Almeshqab, F.; Ustun, T.S. Lessons learned from rural electrification initiatives in developing countries: Insights for technical, social, financial and public policy aspects. *Renew. Sustain. Energy Rev.* **2019**, *102*, 35–53. [CrossRef]

2. Ciller, P.; Lumbreras, S. Electricity for all: The contribution of large-scale planning tools to the energy-access problem. *Renew. Sustain. Energy Rev.* **2020**, *120*, 109624. [CrossRef]

3. Edwin, M.; Nair, M.S.; Joseph Sekhar, S. A comprehensive review for power production and economic feasibility on hybrid energy systems for remote communities. *Int. J. Ambient Energy* **2020**, 1–39. [CrossRef]

4. Taebnia, M.; Heikkilä, M.; Mäkinen, J.; Kiukkonen-Kivioja, J.; Pakanen, J.; Kurnitski, J. A qualitative control approach to reduce energy costs of hybrid energy systems: Utilizing energy price and weather data. *Energies* **2020**, *16*, 1401. [CrossRef]

5. Zhao, H.; Lu, H.; Li, B.; Wang, X.; Zhang, S.; Wang, Y. Stochastic optimization of microgrid participating day-ahead market operation strategy with consideration of energy storage system and demand response. *Energies* **2020**, *13*, 1255. [CrossRef]

6. Wang, Y.; Yang, Y.; Tang, L.; Sun, W.; Zhao, H. A stochastic-CVaR optimization model for CCHP micro-grid operation with consideration of electricity market, wind power accommodation and multiple demand response programs. *Energies* **2019**, *12*, 3983. [CrossRef]

7. Wang, Y.; Huang, Y.; Wang, Y.; Yu, H.; Li, R.; Song, S. Energy management for smart multi-energy complementary micro-grid in the presence of demand response. *Energies* **2018**, *11*, 974. [CrossRef]

8. Nguyen, A.D.; Bui, V.H.; Hussain, A.; Nguyen, D.H.; Kim, H.M. Impact of demand response programs on optimal operation of multi-microgrid system. *Energies* **2018**, *11*, 1452. [CrossRef]

9. Ahmad, S.; Ahmad, A.; Naeem, M.; Ejaz, W.; Kim, H.S. A compendium of performance metrics, pricing schemes, optimization objectives, and solution methodologies of demand side management for the smart grid. *Energies* **2018**, *11*, 2801. [CrossRef]

10. Zunnurain, I.; Maruf, M.; Islam, N.; Rahman, M.; Shafiullah, G. Implementation of advanced demand side management for microgrid incorporating demand response and home energy management system. *Infrastructures* **2018**, *3*, 50. [CrossRef]

11. Hussain, H.M.; Javaid, N.; Iqbal, S.; Hasan, Q.U.; Aurangzeb, K.; Alhussein, M. An efficient demand side management system with a new optimized home energy management controller in smart grid. *Energies* **2018**, *11*, 190. [CrossRef]

12. Wang, Y.; Tang, Y.; Xu, Y.; Xu, Y. A Distributed Control Scheme of Thermostatically Controlled Loads for the Building-Microgrid Community. *IEEE Trans. Sustain. Energy* **2020**, *11*, 350–360. [CrossRef]

13. Wang, Y.; Xu, Y.; Tang, Y. Distributed aggregation control of grid-interactive smart buildings for power system frequency support. *Appl. Energy* **2019**, *251*, 113371. [CrossRef]

14. Franz, M.; Peterschmidt, N.; Rohrer, M.; Kondev, B. *Mini-Grid Policy Toolkit*; Technical Report; Alliance for Rural Electrification: Eschborn, Germany, 2014.

15. Reber, T.; Booth, S.; Cutler, D.; Li, X.; Salasovich, J.; Ratterman, W. *Tariff Considerations for Micro-Grids in Sub-Saharan Africa*; Technical Report February; NREL: Golden, CO, USA, 2018.

16. Casillas, C.E.; Kammen, D.M. The delivery of low-cost, low-carbon rural energy services. *Energy Policy* **2011**, *39*, 4520–4528. [CrossRef]

17. Jin, M.; Feng, W.; Liu, P.; Marnay, C.; Spanos, C. MOD-DR: Microgrid optimal dispatch with demand response. *Appl. Energy* **2017**, *187*, 758–776. [CrossRef]

18. Kahrobaee, S.; Asgarpoor, S.; Qiao, W. Optimum sizing of distributed generation and storage capacity in smart households. *IEEE Trans. Smart Grid* **2013**, *4*, 1791–1801. [CrossRef]

19. Erdinc, O.; Paterakis, N.G.; Pappi, I.N.; Bakirtzis, A.G.; Catalão, J.P. A new perspective for sizing of distributed generation and energy storage for smart households under demand response. *Appl. Energy* **2015**, *143*, 26–37. [CrossRef]

20. Kerdphol, T.; Qudaih, Y.; Mitani, Y. Optimum battery energy storage system using PSO considering dynamic demand response for microgrids. *Int. J. Electr. Power Energy Syst.* **2016**, *83*, 58–66. [CrossRef]

21. Nojavan, S.; Majidi, M.; Esfetanaj, N.N. An efficient cost-reliability optimization model for optimal siting and sizing of energy storage system in a microgrid in the presence of responsible load management. *Energy* **2017**, *139*, 89–97. [CrossRef]

22. Majidi, M.; Nojavan, S.; Zare, K. Optimal Sizing of Energy Storage System in a Renewable-Based Microgrid Under Flexible Demand Side Management Considering Reliability and Uncertainties. *J. Oper. Autom. Power Eng.* **2017**, *5*, 205–214.

23. Amir, V.; Jadid, S.; Ehsan, M. Optimal Planning of a Multi-Carrier Microgrid (MCMG) Considering Demand-Side Management. *Int. J. Renew. Energy Res.* **2018**, *8*, 238–249.

24. Clairand, J.M.; Arriaga, M.; Canizares, C.A.; Alvarez-Bel, C. Power Generation Planning of Galapagos' Microgrid Considering Electric Vehicles and Induction Stoves. *IEEE Trans. Sustain. Energy* **2019**, *10*, 1916–1926. [CrossRef]

25. Gamarra, C.; Guerrero, J.M. Computational optimization techniques applied to microgrids planning: A review. *Renew. Sustain. Energy Rev.* **2015**, *48*, 413–424. [CrossRef]

26. Khodaei, A.; Bahramirad, S.; Shahidehpour, M. Microgrid Planning Under Uncertainty. *IEEE Trans. Power Syst.* **2015**, *30*, 2417–2425. [CrossRef]

27. Chauhan, A.; Saini, R.P. Size optimization and demand response of a stand-alone integrated renewable energy system. *Energy* **2017**, *124*, 59–73. [CrossRef]

28. Amrollahi, M.H.; Bathaee, S.M.T. Techno-economic optimization of hybrid photovoltaic/wind generation together with energy storage system in a stand-alone micro-grid subjected to demand response. *Appl. Energy* **2017**, *202*, 66–77. [CrossRef]

29. Mehra, V.; Amatya, R.; Ram, R.J. Estimating the value of demand-side management in low-cost, solar micro-grids. *Energy* **2018**, *163*, 74–87. [CrossRef]

30. Mehra, V. Optimal Sizing of Solar and Battery Assets in Decentralized Micro-Grids with Demand-Side Management. Ph.D. Thesis, Massachusetts Institute of Technology: Cambridge, MA, USA, 2017.

31. Harper, M. *Review of Strategies and Technologies for Demand-Side Management on Isolated Mini-Grids*; Technical Report; Lawrence Berkeley National Laboratory, Schatz Energy Research Center: Berkeley, CA, USA, 2013.

32. Prathapaneni, D.R.; Detroja, K.P. An integrated framework for optimal planning and operation schedule of microgrid under uncertainty. *Sustain. Energy Grids Netw.* **2019**, *19*, 100232. [CrossRef]

33. Luo, X.; Liu, J.; Liu, Y.; Liu, X. Bi-level optimization of design, operation, and subsidies for standalone solar/diesel multi-generation energy systems. *Sustain. Cities Soc.* **2019**, *48*, 101592. [CrossRef]

34. Kiptoo, M.K.; Adewuyi, O.B.; Lotfy, M.E.; Ibrahimi, A.M.; Senjyu, T. Harnessing demand-side management benefit towards achieving a 100% renewable energy microgrid. *Energy Rep.* **2020**, *6*, 680–685. [CrossRef]

35. Rehman, S.; Habib, H.U.R.; Wang, S.; Buker, M.S.; Alhems, L.M.; Al Garni, H.Z. Optimal Design and Model Predictive Control of Standalone HRES: A Real Case Study for Residential Demand Side Management. *IEEE Access* **2020**, *8*, 29767–29814. [CrossRef]

36. Choynowski, P. *Measuring Willingness to Pay for Electricity*; Technical Report 3; Asian Development Bank: Manila, Philippines, 2002.

37. Oerlemans, L.A.; Chan, K.Y.; Volschenk, J. Willingness to pay for green electricity: A review of the contingent valuation literature and its sources of error. *Renew. Sustain. Energy Rev.* **2016**, *66*, 875–885. [CrossRef]

38. Kim, J.H.; Lim, K.K.; Yoo, S.H. Evaluating residential consumers' willingness to pay to avoid power outages in South Korea. *Sustainability* **2019**, *11*, 1258. [CrossRef]

39. Yevdokimov, Y.; Getalo, V.; Shukla, D.; Sahin, T. Measuring willingness to pay for electricity: The case of New Brunswick in Atlantic Canada. *Energy Environ.* **2019**, *30*, 292–303. [CrossRef]

40. Ali, A.; Kolter, J.Z.; Diamond, S.; Boyd, S. Disciplined convex stochastic programming: A new framework for stochastic optimization. In Proceedings of the Thirty-First Conference on Uncertainty in Artificial Intelligence, Amsterdam, The Netherlands, 12–16 July 2015; Number 3 in 31, pp. 62–71.

41. Liberti, L.; Maculan, N. Disciplined Convex Programming. In *Global Optimization, from Theory to Implementation*; Springer: Berlin/Heidelberg, Germany, 2008; Volume 105, pp. 9455–9456. [CrossRef]

42. Celik, B.; Roche, R.; Suryanarayanan, S.; Bouquain, D.; Miraoui, A. Electric energy management in residential areas through coordination of multiple smart homes. *Renew. Sustain. Energy Rev.* **2017**, *80*, 260–275. [CrossRef]

43. Inversin, A.R. *Mini-Grid Design Manual (English)*; Technical Report; World Bank: Washington, DC, USA, 2000.

44. Baatz, B. *Rate Design Matters: The Intersection of Residential Rate Design and Energy Efficiency*; Technical Report March; American Council for an Energy-Efficient Economy: Washington, DC, USA, 2017.

45. Glick, D.; Lehrman, M.; Smith, O. *Rate Design for the Distribution Edge*; Technical Report August; Rocky Mountain Institute: Boulder, CO, USA, 2014.

46. Kostková, K.; Omelina.; Kyčina, P.; Jamrich, P. An introduction to load management. *Electr. Power Syst. Res.* **2013**, *95*, 184–191. [CrossRef]

47. Joe-Wong, C.; Sen, S.; Ha, S.; Chiang, M. Optimized day-ahead pricing for smart grids with device-specific scheduling flexibility. *IEEE J. Sel. Areas Commun.* **2012**, *30*, 1075–1085. [CrossRef]

48. Borenstein, S.; Jaske, M.; Rosenfeld, A. *Dynamic Pricing , Advanced Metering and Demand Response in Electricity Markets*; Technical Report October; University of California Energy Institute: Berkeley, CA, USA, 2002.

49. Liberti, L.; Maculan, N. *Global Optimization: From Theory to Implementation*; Springer: Berlin/Heidelberg, Germany, 2006; pp. 155–210.

50. Diamond, S.; Boyd, S. CVXPY: A Python-embedded modeling language for convex optimization. *J. Mach. Learn. Res.* **2016**, *17*, 1–5.

51. Andersen, E.D.; Roos, C.; Terlaky, T. On implementing a primal-dual interior-point method for conic quadratic optimization. *Math. Program. Ser. B* **2003**, *95*, 249–277. [CrossRef]

52. Andersen, E.D.; Andersen, K.D. The Mosek Interior Point Optimizer for Linear Programming: An Implementation of the Homogeneous Algorithm. In *High Performance Optimization*; Frenk, H., Roos, K., Terlaky, T., Zhang, S., Eds.; Springer: Boston, MA, USA, 2000; Volume 33, doi:10.1007/978-1-4757-3216-0. [CrossRef]

53. Oviedo Cepeda, J.C.; Khalatbarisoltani, A.; Boulon, L.; Osma-pinto, A.; Antonio, C.; Gualdron, D.; Solano, J.E. Design of an Incentive-based Demand Side Management Strategy for Stand-Alone Microgrids Planning. *Int. J. Sustain. Energy Plan. Manag.* **2020**, *28*, 1–21. [CrossRef]

54. Li, B.; Roche, R.; Paire, D.; Miraoui, A. Sizing of a stand-alone microgrid considering electric power, cooling/heating, hydrogen loads and hydrogen storage degradation. *Appl. Energy* **2017**, *205*, 1244–1259. [CrossRef]

55. Zhang, J.; Li, K.J.; Wang, M.; Lee, W.J.; Gao, H.; Zhang, C.; Li, K. A Bi-Level Program for the Planning of an Islanded Microgrid Including CAES. *IEEE Trans. Ind. Appl.* **2016**, *52*, 2768–2777. [CrossRef]

56. Skoplaki, E.; Palyvos, J.A. Operating temperature of photovoltaic modules: A survey of pertinent correlations. *Renew. Energy* **2009**, *34*, 23–29. [CrossRef]

57. Bukar, A.L.; Tan, C.W.; Lau, K.Y. Optimal sizing of an autonomous photovoltaic/wind/battery/diesel generator microgrid using grasshopper optimization algorithm. *Sol. Energy* **2019**, *188*, 685–696. [CrossRef]

58. Grupo EPM. *Tarifas de Energía Mercado Regulado*; Grupo EPM: Medellín, Colombia, 2019.